Vol 14 No 4, April 2005
1009-1963/2005/14(04)/0690-07

Chinese Physics

© 2005 Chin. Phys. Soc.
and IOP Publishing Ltd

Evolution of spin-dependent atomic wave packets in a harmonic potential*

Wen Ling-Hua(文灵华)[a)b)c)†], Liu Min(刘 敏)[a)b)c)], Kong Ling-Bo(孔令波)[a)b)c)], Chen Ai-Xi(陈爱喜)[a)b)c)], and Zhan Ming-Sheng (詹明生)[a)b)‡]

[a)] *State Key Laboratory of Magnetic Resonance and Atomic and Molecular Physics, Wuhan Institute of Physics and Mathematics, Chinese Academy of Sciences, Wuhan* 430071, *China*
[b)] *Centre for Cold Atom Physics, Chinese Academy of Sciences, Wuhan* 430071, *China*
[c)] *Graduate School, Chinese Academy of Sciences, Wuhan* 430071, *China*

(Received 10 October 2004; revised manuscript received 6 November 2004)

We have investigated theoretically the evolution of spin-dependent atomic wave packets in a harmonic magnetic trapping potential. For a Bose-condensed gas, which undergoes a Mott insulator transition and a spin-dependent transport, the atomic wavefunction can be described by an entangled single-atom state. Due to the confinement of the harmonic potential, the density distributions exhibit periodic decay and revival, which is different from the case of free expansion after switching off the combined harmonic and optical lattice potential.

Keywords: Bose–Einstein condensate, density distribution, spin-dependent optical lattice, magnetic trap
PACC: 0530J, 0560, 4210J

1. Introduction

Since the first experimental realization of Bose–Einstein condensates (BECs) in the dilute alkali-atomic gases,[1−3] there have been intensive theoretical and experimental studies on different aspects of the condensates.[4−13] Recently, much attention has been paid to the investigation of BECs and degenerate Fermi gases in optical lattices.[14−20] The periodic potential of a standing-wave laser field provides a controllable test-bed to investigate the unique properties of the BECs and a flexible tool to manipulate the ultra-cold atoms for the sake of quantum information processing.[21] In general, interference patterns are used as a dominant probe of these systems in experiment because the sizes of the BECs in most experiments are much too small (of order of mm). Actually, the interference patterns resulting from the expansion of an array of subcondensates formed in an optical lattice were crucial in the confirmation of coherence,[22] phase diffusion,[23] number squeezing,[24] Bloch oscillation and Landau–Zener tunnelling,[25] Mott insulator transition,[15,26] and coherent state revivals.[16]

In a recent experiment,[27] Mandel *et al* developed an effective technique of spin-dependent transport to split and transport selectively the atomic wave packets in a one-dimensional (1D) optical lattice. Briefly, after the system reaches the Mott insulating phase[15] one turns off the magnetic trap and the optical lattices along the y and z directions. Consequently, there only exists a 1D spin-dependent optical lattice along the x direction that is created by two counterpropagating laser beams with linear polarization vectors enclosing an angleθ. By changing the polarization angle θ one can realize the splitting of the atomic wave packets such that the wave packets of an atom in spin states $|0\rangle \equiv |F=1, m_{\rm F}=-1\rangle$ and $|1\rangle \equiv |F=2, m_{\rm F}=-2\rangle$, respectively, are transported in opposite directions, which is the so-called spin-dependent transport (coherent transport). Finally, the optical lattice is switched off and the coherence of the transport is demonstrated by the observed high contrast interference patterns.

*Project supported by the National Natural Science Foundation of China (Grant Nos 10474119 and 10474117), by the National Fundamental Research Programme of China (Grant No 001CB309309), and also by funds from the Chinese Academy of Sciences.
†E-mail: wenlinghua@wipm.ac.cn
‡E-mail: mszhan@wipm.ac.cn

In our recent work,[28] we have presented a theoretical model to study the free expansion of spin-dependent atomic wave packets after switching off the magnetic trap and the optical lattice. The theoretical results agree well with the interference patterns observed in the experiment.[27] In this paper, we generalize the model to investigate the evolution of the spin-dependent atomic wave packets under the action of a harmonic potential. The difference between our present scheme and the experiment[27] is that here an axially symmetric magnetic trap is maintained. After a coherent transport, the system is confined in a 1D spin-dependent optical lattice and a magnetic trap with an axial symmetry along the x direction. Once the optical lattice is switched off, the spin-dependent atomic wave packets emanating from different lattice sites expand and overlap, which results in a clear interference pattern after a time of flight (TOF). It is shown that the evolution of the interference patterns in a harmonic potential exhibits a periodic oscillation of decay and revival. On the one hand, our experimental proposal provides a new way to further test our recent work[28] and prediction. On the other hand, as the system undergoes a Mott insulator transition and a spin-dependent transport before the removal of the optical lattice, the evolution of the density distribution (i.e., the evolution of interference pattern) in the harmonic potential is more complicated than that of the common cases,[29−32] which is helpful to the exploration of the physical essence of interference.

2. The model of density distribution in a harmonic potential

For a Bose–Einstein condensate trapped in a combined harmonic and 3D optical lattice potential, the atoms are localized on individual lattice sites with no phase coherence when it enters the Mott insulating phase. After releasing the optical lattices along the y and z directions, there is an array of subcondensates formed in the 1D spin-dependent optical lattice along the horizontal x direction where the effective angular frequency is $\tilde{\omega}_x = 2\pi \times 45\text{kHz}$.[27] Then we let the axial magnetic field remain along the x direction and weaken the radial magnetic fields along the y and z directions such that the axial and radial angular frequencies of the harmonic potential are given by $\omega_x = 2\pi \times 16\text{Hz}$ and $\omega_\perp = \pi\text{Hz}$, respectively. The chemical potential in the central lattice site of the system can be expressed by $\mu_0 = m\omega_x^2 d^2 k_M^2/2$, where m is the mass of ^{87}Rb atom, $d = \lambda/2$ is the period of the optical lattice, and $2k_M+1$ represents the total number of lattice sites. In this situation, the system satisfies the condition $\hbar\omega_\perp \ll \mu_0 \ll \hbar\tilde{\omega}_x$, which can be seen clearly in the next section ($d = 392.5\text{nm}$, $k_M \sim 12$). Thus, when the evolution of the spin-dependent atomic wave packets in the magnetic trap is investigated in the x direction after the optical lattice is switched off, the non-interacting model can give a well description as the above condition is satisfied.[22,29]

In the presence of a magnetic trap, the number of atoms in different individual lattice sites should be different. The ratio between the atomic number N_k in the kth lattice site and the total number of the condensed atoms N is given by $N_k/N = 15(1 - k^2/k_M^2)^2/16k_M$.[22] Since each subcondensate confined in the joint harmonic and 1D spin-dependent optical lattice potential is fully coherent, it can be described by a single order parameter $\Psi_k = N_k^{1/2}\phi_k$ according to the Hartree or mean-field approximation,[33] where ϕ_k is the single-particle wavefunction in the kth lattice site.

We consider an atom with two hyperfine states $|0\rangle$ and $|1\rangle$ forming the logical bases of a single atom at each lattice site. Initially, the atom lies in spin state $|0\rangle_k$ where the subscript denotes the kth lattice site. The following analysis is similar to the method developed in our recent work.[28] By using a $\pi/2$ microwave pulse to drive Rabi oscillations between the two hyperfine states, the atom can be placed into a coherent superposition of the two internal states $|0\rangle_k$and $|1\rangle_k$,

$$|0\rangle_k \xrightarrow{\pi/2} \frac{1}{\sqrt{2}}(|0\rangle_k + i\,|1\rangle_k),$$
$$|1\rangle_k \xrightarrow{\pi/2} \frac{1}{\sqrt{2}}(\mathrm{i}\,|0\rangle_k + |1\rangle_k). \quad (1)$$

After a spin-dependent transport, the atomic wavefunction can be described by an entangled single-atom state, i.e. an entangled quantum state between the internal degree of freedom (spin) and the spatial degree of freedom (spatial wave packet)

$$\psi_k = \frac{1}{\sqrt{2}}(|0\rangle_k \varphi_k + \mathrm{i}\,\exp[\mathrm{i}\beta]\,|0\rangle_{k+r} \varphi_{k+r}), \quad (2)$$

where β is the relative phase between the two wave packets, which is obtained in the transport; r denotes the separation between the two spin-dependent wave packets that originate from the same lattice site. By applying a final $\pi/2$ microwave pulse whose transform rule is given by Eq.(1), one has

$$\phi_k = |0\rangle\,\Xi_{0,k} + |1\rangle\,\Xi_{1,k} \quad (3)$$

where $\Xi_{0,k}$ and $\Xi_{1,k}$ are respectively given by

$$\Xi_{0,k} = \frac{A}{2}\left(\exp\left[-\frac{(x-kd)^2}{2\sigma^2}\right] - \exp\left[\mathrm{i}\beta - \frac{(x-(k+r)d)^2}{2\sigma^2}\right]\right), \quad (4)$$

$$\Xi_{1,k} = \frac{\mathrm{i}A}{2}\left(\exp\left[-\frac{(x-kd)^2}{2\sigma^2}\right] + \exp\left[\mathrm{i}\beta - \frac{(x-(k+r)d)^2}{2\sigma^2}\right]\right); \quad (5)$$

$A = 1/\sigma^{1/2}\pi^{1/4}$ is a normalization constant and σ denotes the width of the subcondensate in each lattice site. In Eq.(3), we have assumed a Gaussian approximation in coordinate space for the spatial wave packets, and the subscripts of spin states $|0\rangle$ and $|1\rangle$ are removed on account of the bosonic identity.

When the spin-dependent optical lattice is switched off, the evolution of the spatial components $\Xi_{j,k}(x,t)(j=0,1)$ of the atomic wavefunction can be derived by the propagator method[29,30,34,35]

$$\Xi_{j,k}(x,t) = \int_{-\infty}^{\infty} K(x,t;y,t=0)\Xi_{j,k}(y,t=0)\mathrm{d}y, \quad (6)$$

where $\Xi_{j,k}(y,t=0)(j=0,1)$ are the spatial wavefunctions of spin states at the initial time $t=0$, which are given by Eqs.(4) and (5), and $K(x,t;y,t=0)$ is the propagator in a harmonic potential, expressed as

$$K(x,t;y,t=0) = \left[\frac{m\omega_x}{2\pi\mathrm{i}\hbar\sin\omega_x t}\right]^{1/2} \times \exp\left\{\frac{\mathrm{i}m\omega_x}{2\pi\sin\omega_x t}[(x^2+y^2)\times\cos\omega_x t - 2xy]\right\}. \quad (7)$$

By combining Eqs.(4)–(7), one can obtain the following analytical results of the spatial components after a straightforward calculation:

$$\begin{aligned}\Xi_{0,k} =& \frac{A}{2}\sqrt{\frac{1}{\sin\omega_x t(\cot\omega_x t+\mathrm{i}\gamma)}}\left\{\exp\left[-\frac{(kd\cos\omega_x t-x)^2}{2\sigma^2\sin^2\omega_x t(\cot^2\omega_x t+\gamma^2)}\right]\right.\\ &\times\exp\left[-\frac{\mathrm{i}(kd\cos\omega_x t-x)^2\cot\omega_x t}{2\gamma\sigma^2\sin^2\omega_x t(\cot^2\omega_x t+\gamma^2)}\right]\exp\left[\frac{\mathrm{i}(x^2\cos\omega_x t+k^2d^2\cos\omega_x t-2xkd)}{2\gamma\sigma^2\sin^2\omega_x t}\right]\\ &-\exp\left[\mathrm{i}\beta-\frac{((k+r)d\cos\omega_x t-x)^2}{2\sigma^2\sin^2\omega_x t(\cot^2\omega_x t+\gamma^2)}\right]\exp\left[-\frac{\mathrm{i}((k+r)d\cos\omega_x t-x)^2\cot\omega_x t}{2\gamma\sigma^2\sin^2\omega_x t(\cot^2\omega_x t+\gamma^2)}\right]\\ &\left.\times\exp\left[\frac{\mathrm{i}(x^2\cos\omega_x t+(k+r)^2d^2\cos\omega_x t-2x(k+r)d)}{2\gamma\sigma^2\sin^2\omega_x t}\right]\right\}, \end{aligned} \quad (8)$$

$$\begin{aligned}\Xi_{1,k} =& \frac{\mathrm{i}A}{2}\sqrt{\frac{1}{\sin\omega_x t(\cot\omega_x t+\mathrm{i}\gamma)}}\left\{\exp\left[-\frac{(kd\cos\omega_x t-x)^2}{2\sigma^2\sin^2\omega_x t(\cot^2\omega_x t+\gamma^2)}\right]\right.\\ &\times\exp\left[-\frac{\mathrm{i}(kd\cos\omega_x t-x)^2\cot\omega_x t}{2\gamma\sigma^2\sin^2\omega_x t(\cot^2\omega_x t+\gamma^2)}\right]\exp\left[\frac{\mathrm{i}(x^2\cos\omega_x t+k^2d^2\cos\omega_x t-2xkd)}{2\gamma\sigma^2\sin^2\omega_x t}\right]\\ &+\exp\left[\mathrm{i}\beta-\frac{((k+r)d\cos\omega_x t-x)^2}{2\sigma^2\sin^2\omega_x t(\cot^2\omega_x t+\gamma^2)}\right]\exp\left[-\frac{\mathrm{i}((k+r)d\cos\omega_x t-x)^2\cot\omega_x t}{2\gamma\sigma^2\sin^2\omega_x t(\cot^2\omega_x t+\gamma^2)}\right]\\ &\left.\times\exp\left[\frac{\mathrm{i}(x^2\cos\omega_x t+(k+r)^2d^2\cos\omega_x t-2x(k+r)d)}{2\gamma\sigma^2\sin^2\omega_x t}\right]\right\}, \end{aligned} \quad (9)$$

with the dimensionless parameter $\gamma = \hbar/m\omega_x\sigma^2$.

We now consider the density distribution of the spin-dependent atomic wave packets (i.e., the density distribution of the whole condensate) under the action of the harmonic potential. Obviously, there is no correlation between the atomic wave packets in different spin states as the two logical basis-vectors $|0\rangle$ and $|1\rangle$are orthogonal. Thus for the subcondensate initially confined in the jth lattice site, the density distributions of the atomic wave packets in spin states $|0\rangle$ and $|1\rangle$, respectively, are given by

$$n_{0,k}(x,t) = N_k\left|\Xi_{0,k}(x,t)\right|^2, \quad (10)$$

$$n_{1,k}(x,t) = N_k\left|\Xi_{1,k}(x,t)\right|^2, \quad (11)$$

with $N_k = 15N(1-k^2/k_M^2)^2/16k_M$. In the above Eqs.(10) and (11), we have taken into account the well coherence between the delocalized wave packets of the same atom, which originates from the entanglement

of a single atom. Since the system undergoes a Mott insulator transition before the spin-dependent transport, there is no correlation between the wave packets of the same spin state that are split out from different original lattice sites. So, after the optical lattice is switched off, the density distributions of the wave packets in states $|0\rangle$ and $|1\rangle$, i.e. the density distributions of the overall subcondensates in the total lattice sites, can be expressed as

$$n_0(x,t) = \sum_{k=-k_M}^{k_M} n_{0,k}(x,t), \tag{12}$$

$$n_1(x,t) = \sum_{k=-k_M}^{k_M} n_{1,k}(x,t). \tag{13}$$

3. Numerical results

In the following calculations, we use the experimental parameters where $N = 3\times10^5$,$\omega_x = 2\pi\times16$Hz, $\omega_\perp = \pi$Hz, $\lambda = 785$nm, $d = 392.5$nm.[27] The total number of the lattice sites $2k_M+1$ can be determined theoretically by the formula[19]

$$k_M^2 = \frac{2\hbar\varpi}{m\omega_x^2 d^2}\left(\frac{15}{8\sqrt{\pi}}N\frac{a}{a_{\rm ho}}\frac{d}{\sigma}\right)^{2/5}, \tag{14}$$

where the geometric average $\varpi = (\omega_x\omega_\perp^2)^{1/3}$, the oscillator length $a_{\rm ho} = \sqrt{\hbar/m\varpi}$, and the s-wave scattering length for ^{87}Rb atom is $a \sim 5$nm. Thus $k_M \sim 12$ is obtained from the above equation. Since the value of σ, which characterizes the width of the subcondensate in each lattice site, is chiefly determined by the optical confinement, one can evaluate it in terms of a variational calculation minimizing the energy of the condensate. As a result, the ratio is given by $\sigma/d = 0.16$. According to our recent work, the relative phase β is almost constant throughout the cloud of atoms and its absolute value is small.[28] For simplicity, we treat it as zero.

3.1. Periodic decay and revival of the density

From Eqs.(8) and (9), the density distributions $n_j(x,t)$ $(j = 0,1)$ of the atomic wave packets in the x direction should exhibit periodic character with a period of $T = \pi/\omega_x$. For the experimental parameters mentioned above, $\omega_x = 2\pi\times16$Hz, which means $T = 31.25$ms. Displayed in Fig.1 is the density $n_1(x=0,t)$ of the spin-1 wave packets (i.e., the density of the atomic wave packets in state $|1\rangle$) at $x = 0$ versus time t, where initially localized atoms have been delocalized over two lattice sites and the separation is denoted by r. It is shown clearly that there is a periodic decay and revival oscillation of the density, which results from the confinement of the harmonic potential. The periodicity embodied in Fig.1 is in agreement with the analytical result $T = 31.25$ms.

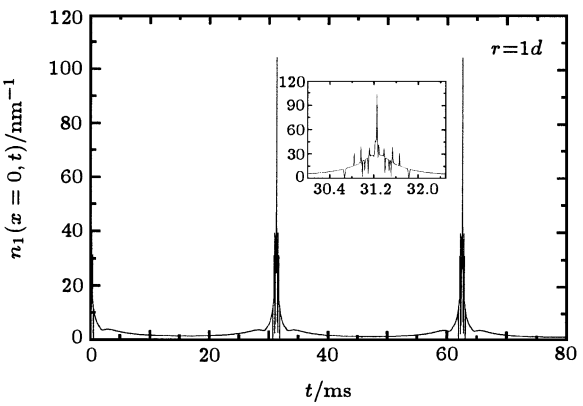


Fig.1. Density of the spin-1 wave packets at $x = 0$ versus time t, under the action of a harmonic potential. The initially localized atoms have been delocalized over two lattice sites. The density $n_1(x=0,t)$ is given in units of nm^{-1}, r denotes the separation between the two wave packets of an atom after a spin-dependent transport.

3.2. Density distributions of spin-1 wave packets

For the sake of contrast, we consider the density distributions of the spin-1 wave packets after the optical lattice is switched off, with the time of flight being 14ms. The analytical result at time t is given by Eq.(13). Shown in Fig.2(a) is the density distribution (in units of nm^{-1}) in state $|1\rangle$ at $t = 14$ms after the initially localized atoms have been delocalized over two lattice sites. In the following figures plotted in this paper, the horizontal coordinate x is in units of μm and the vertical coordinate is in units of nm^{-1}. The density distributions in the cases that the initially localized atoms have been delocalized over three (b), four (c), five (d), six (e), and seven (f) lattice sites are also given in Fig.2.

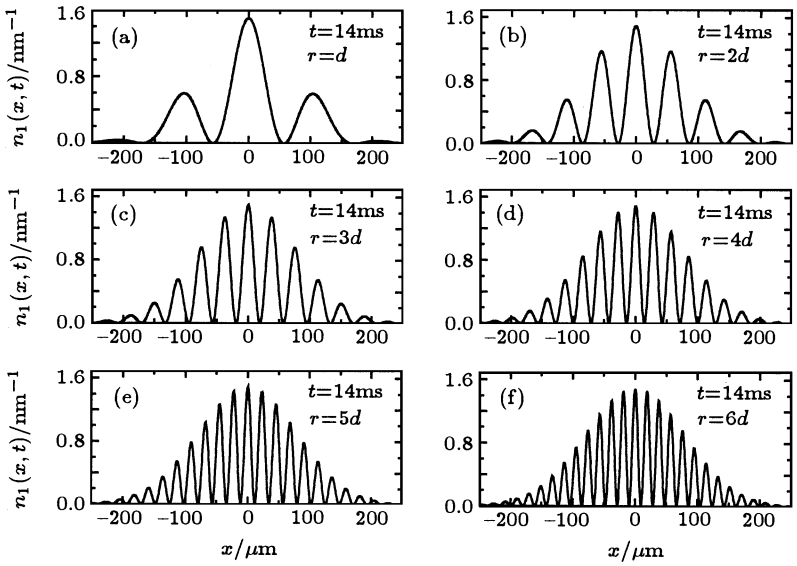


Fig.2. Density distributions of spin-1 wave packets under the action of a harmonic potential in the cases that the initially localized atoms have been delocalized over two (a), three (b), four (c), five (d), six (e), and seven (f) lattice sites. The time of flight is 14ms. The vertical coordinate $n_1(x,t)$is in units of nm^{-1} and the horizontal coordinate x is in units of μm.

With increasing r, one can see that the interference peak number increases while the fringe spacing of the interference patterns decreases further and the visibility of the interference patterns reduces distinctly. On the other hand, we find that the minimum of each interference peak in the interference patterns is zero, which is different from the case of the combined potential being switched off.[27,28]

3.3. Evolution of the density distribution

In Fig.2, we have given the density distributions in state $|1\rangle$ at $t = 14$ms. However, it is hard to discriminate the free expansion of the atomic wave packets from the expansion under the action of harmonic potential only in terms of the interference peak number and the visibility of the interference patterns. In this context, we plot the evolution of the density distribution of spin-1 wave packets in Fig.3, where the initially localized atoms have been delocalized over three lattice sites by using a $\pi/2 - \pi - \pi/2$ microwave pulse sequence.

From Fig.3, we find that the evolution of the density distribution exhibits a periodic behaviour with a period of $T = 31.25$ms, which is in accord with the analytical result in Eqs.(8) and (9). Shown in Fig.3(c) is the density distribution of spin-1 wave packets at time $t = 15$ms. In contrast to the interference patterns resulting from the free expansion of the atomic wave packets, we can see clearly here the minimum of each interference peak is zero (see Fig.3(c)), which in turn provides a way to test our theoretical model in future possible experiments.

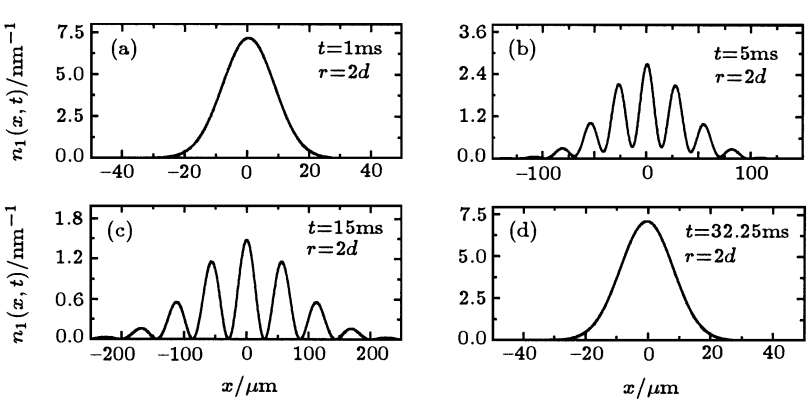


Fig.3. Evolution of the density distribution in state $|1\rangle$ with time t, under the action of a harmonic potential in the case that initially localized atoms have been delocalized over three lattice sites. The density distributions are shown at t =1ms (a), 5ms (b), 15ms (c), and 32.25ms (d).

3.4. Density distributions of spin-0 wave packets

Now we discuss the density distribution of spin-0 wave packets (i.e., density distribution of the atomic wave packets in state $|0\rangle$). Similar to the foregoing analysis, the analytical result of the density distributions in state $|0\rangle$ is given by Eq.(12). In contrast with the interference patterns in state $|1\rangle$, the positions of the sharp peaks in Figs.4(a)–(f) become those of local minimum densities in the density distributions shown in Figs.2(a)–(f), and vice versa, which can be interpreted by the conservation of energy and particle number.

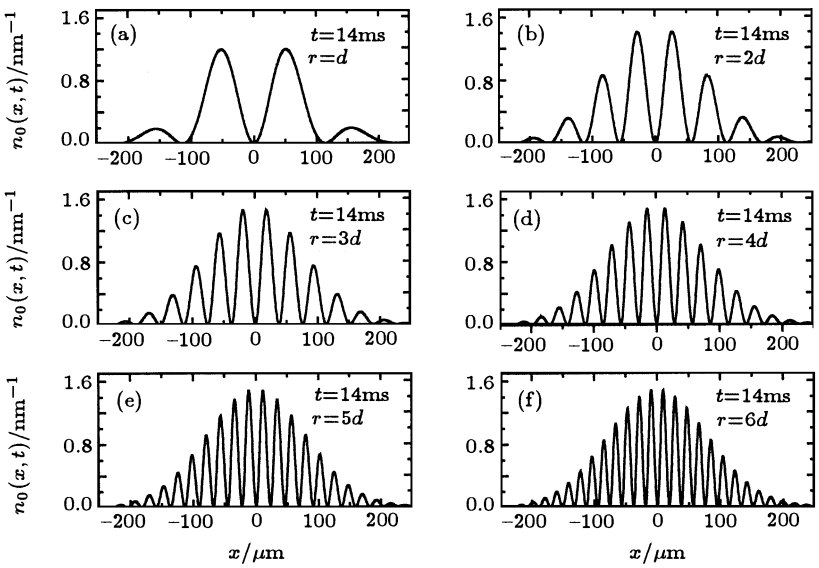


Fig.4. Density distributions of spin-0 wave packets under the action of a harmonic potential in the case that the initially localized atoms have been delocalized over two (a), three (b), four (c), five (d), six (e), and seven (f) lattice sites. The time of flight is 14ms. The vertical coordinate $n_0(x,t)$is in units of nm^{-1} and the horizontal coordinate x is in units of μm.

4. Conclusion

In conclusion, we have investigated the density distributions and evolution of the spin-dependent atomic wave packets in a magnetic trap. After a spin-dependent transport, the atomic wavefunction can be well described by an entangled single-atom state between the internal degree of freedom (spin) and the spatial degree of freedom (spatial wave packet). In the presence of the harmonic potential, we find that the density distribution exhibits a periodic decay and revival (see Fig.1). In contrast with the interference patterns resulting from the free expansion, the minimum of each interference peak in the density distribution at $t = 15$ms (or $t = 14$ms) becomes zero when the evolution of the atomic wave packets is investigated under the action of a harmonic potential (see Figs.2–4). The unique phenomenon provides a way to test the validity of our theoretical model in the present experimental techniques. In addition, since the system experiences a Mott insulator transition and a spin-dependent transport before the optical lattice is switched off, the evolution of the atomic wave packets in the harmonic potential is much more complicated than that of the common cases,[29−32] which will redound to the exploration of the physics of the interference.

Acknowledgement

The authors sincerely thank Xiong H W, Bloch I, Wang J, Gao K L, and Jiang K J for helpful discussions.

References

[1] Anderson M H *et al* 1995 *Science* **269** 198
[2] Davis K B *et al* 1995 *Phys. Rev. Lett.* **75** 3969
[3] Bradley C C *et al* 1995 *Phys. Rev. Lett.* **75** 1687
[4] Dalfovo F *et al* 1999 *Rev. Mod. Phys.* **71** 463
[5] Leggett A J 2001 *Rev. Mod. Phys.* **73** 307
[6] Cataliotti F S *et al* 2001 *Science* **293** 843

[7] Wu Y, Yang X and Xiao Y 2001 *Phys. Rev. Lett.* **86** 2200
[8] Wu Y, Wang X and Sun C 2000 *Phys. Rev.* A **62** 063603
[9] Xiong H *et al* 2002 *Phys. Rev.* A **65** 033609
[10] Xiong H *et al* 2003 *Phys. Rev.* A **67** 055601
[11] Liu S *et al* 2003 *Phys. Rev.* A **68** 065601
[12] Huang G X 2004 *Chin. Phys.* **13** 1866
[13] Cui H T, Wang L C and Yi X X 2004 *Acta Phys. Sin.* **53** 0991 (in Chinese)
[14] Jaksch D *et al* 1998 *Phys. Rev. Lett.* **81** 3108
[15] Greiner M *et al* 2002 *Nature* **415** 39
[16] Greiner M *et al* 2002 *Nature* **419** 51
[17] Zhang W P*et al* 2002 *Phys. Rev. Lett.* **88** 060401
[18] Liu W M, Wu B and Niu Q 2000 *Phys. Rev. Lett.* **84** 2294
[19] Liu W M *et al* 2002 *Phys. Rev. Lett.* **88** 170408
[20] Viverit L *et al* 2004 *Phys. Rev. Lett.* **98** 110401
[21] Bloch I 2004 *Phys. World* **April** pp.25-29
[22] Pedri P*et al* 2001 *Phys. Rev. Lett.* **87** 220401
[23] Xiong H *et al* 2003 *J. Phys. B: At. Mol. Opt. Phys.* **36** 3315
[24] Orzel C *et al* 2001*Science* **291** 2386
[25] Morsch O *et al* 2001 *Phys. Rev. Lett.* **87** 140402
[26] Wu Y and Yang X 2003 *Phys. Rev.* A **68** 013608
[27] Mandel O *et al* 2003 *Phys. Rev. Lett.* **91** 010407
[28] Wen L, Liu M, Xiong H and Zhan M *Preprint cond-mat*/0409349
[29] Xiong H *et al* 2002 *J. Phys. B: At. Mol. Opt. Phys.* **35** 4863
[30] Liu S *et al* 2003 *J. Phys. B: At. Mol. Opt. Phys.* **36** 2083
[31] Müller J H *et al* 2003 *J. Opt. B: Quantum Semiclass. Opt.* **5** S38
[32] Adhikari S K 2003 *J. Phys. B: At. Mol. Opt. Phys.* **36** 3951
[33] Pethick C J and Smith H 2002 *Bose–Einstein Condensation in Dilute Gases* (Cambridge: Cambridge Univ. Press)
[34] Feynman R P and Hibbs A R 1965 *Quantum Mechanics and Path Integrals* (New York: McGraw-Hill)
[35] Liu S *et al* 2003 *Chin. Phys. Lett.* **20** 1202